Research Article

Solid–liquid phase behaviors of binary mixtures of various partial acylglycerols by differential scanning calorimetry

Latifa Seniorita, Eiji Minami*, Haruo Kawamoto

Graduate School of Energy Science, Kyoto University (Yoshida Honmachi, Sakyo-ku, Kyoto, 606-8501 Japan)

***Correspondence:** ((Eiji Minami, Kyoto University Research Building No. 11 Room 206, Yoshida Honmachi, Sakyo-ku, Kyoto, 606-8501 Japan; **Fax:** +81 (0)75 753 5713; **Email:** minami@energy.kyoto-u.ac.jp))

Running Title: Solid–liquid phase behaviors of binary acylglycerols

Keywords: solid–liquid equilibrium, acylglycerols, differential scanning calorimetry, biodiesel, cold flow properties

Abbreviations:
CF, compound formation;
CFP, cold flow property;
DAG, diacylglycerol;
DSC, differential scanning calorimetry;
FAME, fatty acid methyl ester;
MAG, monoacylglycerol;
NSS, non-solid-solution;
SS, solid-solution;
TAG, triacylglycerol

Abstract

Monoacylglycerol (MAG), diacylglycerol (DAG), and triacylglycerol (TAG) are impurities in biodiesel and a major cause of precipitation at low temperatures owing to their high melting points. Understanding the behavior of such acylglycerols is essential for predicting biodiesel cold flow properties (CFPs). Our previous study on MAG/MAG binary mixtures showed that they tend to solidify by forming molecular compounds, causing complex liquidus curves. In contrast, TAG/TAG mixtures, which have been studied extensively, are commonly eutectic or monotectic systems, in which each component solidifies separately as a pure substance. The present study focuses on binary mixtures of DAG/DAG and different acylglycerol pairs (MAG/DAG, TAG/MAG, and DAG/TAG), and determination of their solid–liquid phase behavior by differential scanning calorimetry. As a result, these mixtures were found to behave as eutectic or monotectic systems with no sign of compound formation, and a simple thermodynamic model called the non-solid-solution model could represent their liquidus curves. As DAG and TAG have lower contents than MAG in biodiesel and they are unlikely to form molecular compounds with MAG, it is suggested that DAG and TAG have little effect on the biodiesel CFPs. Therefore, understanding MAG behavior, especially molecular compound formation, will probably be important for predicting biodiesel CFPs.

Practical applications

Biodiesel has attracted much interest because its blending with conventional fossil diesel has become more standard with biofuel mandates. Saturated acylglycerols, such as monopalmitin and monostearin, found in biodiesel as impurities are considered the main cause of biodiesel solidification. From an energy perspective, the solid–liquid phase behavior of acylglycerols will contribute to building prediction models

for biodiesel cold flow properties. As the current specification standards for cold flow properties are based on fossil diesel and do not consider the characteristics of acylglycerols, this study might lead to a reevaluation of conventional standards.

1 Introduction

Biodiesel (fatty acid methyl esters, FAMEs) is produced by the transesterification of plant oils with methanol. In this reaction, one molecule of triacylglycerol (TAG) is converted into diacylglycerol (DAG), monoacylglycerol (MAG), and free glycerol, producing one FAME molecule in each step (three molecules in total). After the catalyst and glycerol are removed by washing with water, unreacted TAG, and intermediates DAG and MAG, can remain in biodiesel as minor components.

Such acylglycerols, especially those bonded to saturated fatty acids, deteriorate the cold flow properties (CFPs) of biodiesel owing to their high melting points and ready solidification in biodiesel[1,2]. These CFPs, such as the cloud point and cold filter plugging point, are indices of liquid fuel fluidity at low temperatures and fuel performance in cold weather.

The polymorphs of acylglycerols also affect CFPs[3–5]. According to a review by Foubert et al.[6], acylglycerols have several crystal arrangements with different thermal properties and, in general, metastable arrangements are formed by crystallization from the melt, while the most stable arrangement is produced via crystallization in a solvent or crystal transition from the metastable forms. The more stable forms have higher melting points. MAGs have three prominent crystal forms, denoted α, β', and β (melting point (T_m), $\alpha < \beta' < \beta$)[6]. DAGs have two β-types, denoted β_1 and β_2 (T_m, $\beta_1 > \beta_2$), with slightly different thermal properties[6]. TAG polymorphs are the most complex, but monoacid TAGs are reported to have α, β', and β-type crystals (T_m, $\alpha < \beta' < \beta$)[6], the same as MAGs.

Chupka et al. and Yoshidomi et al. reported that MAGs solidify as metastable α-form crystals in biodiesel when cooled rapidly, but transform into the β-form during slow heating or long-term storage[3,5]. Furthermore, biodiesel precipitation can occur even at temperatures above the cloud point[4,7], as the MAG melting point differs depending on its crystal form. The prediction of such complex solidification behavior is essential for biodiesel use.

Efforts to predict CFPs using thermodynamic models have been reported[8–10]. Imahara et al. and Dunn have reported thermodynamic models that correlate well with the experimentally determined cloud point[8,11]. However, their models were developed for biodiesel containing only FAMEs (very pure biodiesel) and did not consider the effects of acylglycerols.

Accordingly, we have previously studied the effect of MAGs on biodiesel CFPs using differential scanning calorimetry (DSC)[5,12]. For mixtures of FAMEs containing one type of MAG, MAG solidification was accurately predicted using the non-solid-solution model[5], in which one solid phase is formed from one chemical component. However, this model was inaccurate for mixtures containing multiple types of MAG, suggesting the formation of a single-phase crystal consisting of multiple MAGs[12], denoted the molecular compound. For such mixtures, the compound formation model was effective[12]. Therefore, whether one solid phase consists of a single component or multiple components is important for predicting biodiesel CFPs.

As compound formation behavior has often been observed in binary MAG/MAG mixtures, confirming whether the same behavior occurs in binary mixtures of other combinations is of interest. TAG/TAG mixtures have been extensively studied and reported to not tend to produce molecular compounds[13], with some exceptions[14]. However, studies on other combinations, such as DAG/DAG, DAG/MAG, TAG/MAG, and DAG/TAG, are limited. In this study, DSC analysis was performed on binary mixtures of acylglycerols mixed in the above combinations to determine whether the components solidify separately or form molecular compounds. Three thermodynamic models were used for prediction and compared with the experimental results to aid this discussion.

2 Materials and methods

2.1 Materials and analytical method

High-purity MAG, DAG, and TAG samples in Table 1 were purchased and used as received without purification. These acylglycerols were mixed in various combinations and ratios to prepare binary mixtures.

DSC (DSC-60, Shimadzu Corp., Kyoto, Japan) analysis was performed to evaluate liquidus and solidus temperatures (liquidus > solidus) of the binary mixtures. A mixture becomes completely liquid above the liquidus and fully solid below the solidus. The liquidus is particularly essential for CFPs because a slight solid phase can even form slightly below the liquidus to clog fuel filters.

For each DSC analysis, approximately 10 mg of the sample was placed in an aluminum-based crimping cell and exposed to a dry nitrogen flow (50 mL/min). The sample was heated until fully melted and then cooled rapidly (−10 °C/min) until the first exothermic peak had ended. This peak indicates the formation of the first solid phase, and fast cooling usually forms metastable acylglycerol crystals: α-type for MAG and TAG, and β_2-type for DAG. The sample was then heated immediately (10 °C/min) and the DSC profile recorded. The liquidus temperature was determined from the peak temperature of the highest endothermic peak, while the solidus was determined from that of the lowest endothermic peak, if observed.

This DSC procedure was intended to prevent the crystal transition of acylglycerols and determine the liquidus temperature of α-type MAG in our previous studies[5,15]. Heating after complete solidification or slower heating causes crystal transitions owing to long heating time, complicating the DSC profiles. Contrary to the intention, DAG and TAG seemed to have transitioned to β_1 and β types during the measurement, respectively, as explained later. Nonetheless, we adopted this procedure to unify the analysis conditions with our previous studies for comparison[5,15].

Each pure material was also measured in the same manner to determine thermal properties. The melting point and enthalpy of fusion were determined from the onset temperature and peak area of the endothermic peak, respectively, and used to calculate thermodynamic models.

For DSC analysis, indium and zinc were used for temperature calibration of the instrument, with α-alumina was used as the reference material during experiments. DSC analysis was conducted three times for each sample, and the mean values were used.

2.2 Thermodynamic models

2.2.1 Solid–liquid equilibrium

The liquidus temperature of the mixture was predicted based on the solid–liquid equilibrium theory. This theory can represent the relationship between the liquidus temperature (T) and the properties of the pure component[16].

$$\frac{\gamma_i^L x_i}{\gamma_i^S z_i} = \exp\left[\frac{\Delta H_{m,i}}{RT_{m,i}}\left(\frac{T-T_{m,i}}{T}\right)\right] \qquad (1)$$

where x_i and z_i are the mole fractions of component i in the liquid and solid phases, respectively. The activity coefficients of component i in liquid and solid phases, γ_i^L and γ_i^S, respectively, represented the non-ideality of the solution. γ_i^L was estimated using a modified universal quasi-chemical functional group activity coefficient model, known as the UNIFAC (Dortmund) model[17], while the solid phase was assumed to be ideal (γ_i^S = 1), as in our previous studies[5,12]. $T_{m,i}$ and $\Delta H_{m,i}$ represent the melting point and enthalpy of fusion of pure component i, respectively.

Two assumptions were adopted to calculate Equation 1, namely, non-solid-solution (NSS) and solid-solution (SS) models. The NSS model assumed that different components were immiscible in one solid phase, consisting of a single component i (z_i = 1). For a binary mixture, Equation 1 can be rearranged to Equations 2 and 3.

$$\gamma_1^L x_1 = \exp\left[\frac{\Delta H_{m,1}}{RT_{m,1}}\left(\frac{T-T_{m,1}}{T}\right)\right] \qquad (2)$$

$$\gamma_2^L x_2 = \exp\left[\frac{\Delta H_{m,2}}{RT_{m,2}}\left(\frac{T-T_{m,2}}{T}\right)\right] \qquad (3)$$

Equations 2 and 3 give two liquidus curves for components 1 and 2, respectively, with their intersection denoted as the eutectic point. These two associate into a V-shaped liquidus curve, known as a eutectic system. However, when the melting point difference between components 1 and 2 is large, the equation with the higher melting point becomes dominant, while the other is almost negligible, and the liquidus line appears as a monotonically increasing curve instead of a V-

shape. This case is known as a monotectic system but essentially the same as eutectic, following the NSS model.

In contrast, the SS model assumed that multiple components can produce a mixed crystal ($z_i \neq 1$) at any ratio. For a binary mixture ($z_1 + z_2 = 1$), Equation 1 can be rearranged to Equation 4.

$$\gamma_1{}^{\mathrm{L}} x_1 / \exp\left[\frac{\Delta H_{m,1}}{RT_{m,1}}\left(\frac{T-T_{m,1}}{T}\right)\right] + \gamma_2{}^{\mathrm{L}} x_2 / \exp\left[\frac{\Delta H_{m,2}}{RT_{m,2}}\left(\frac{T-T_{m,2}}{T}\right)\right] = 1 \qquad (4)$$

This equation produces a monotonically increasing liquidus curve, similar to a monotectic system. Therefore, when the melting point difference is large, the NSS and SS models can hardly be distinguished using only the liquidus curve shape.

2.2.2 Compound formation

When multiple components form a single-phase crystal (molecular compound) at a specific molar ratio, the compound formation (CF) model based on the reaction equilibrium can be used[12]. When v_1 moles of component C_1 and v_2 moles of C_2 in a liquid phase (L) produce one mole of solid compound C_3 in a solid phase (S), the reaction is described as shown in Equation 5:

$$v_1 C_1(L) + v_2 C_2\ (L) \leftrightarrow C_3\ (S) \qquad (5)$$

The solid compound C_3 can be reversibly converted to liquid components C_1 and C_2. These forward and backward reactions are in equilibrium, and the equilibrium constant (K_a) is shown in Equation 6:

$$K_a = \frac{(\gamma_1{}^L x_1)^{v_1}(\gamma_2{}^L x_2)^{v_2}}{(\gamma_3{}^S z_3)^1} = (\gamma_1{}^L x_1)^{v_1}(\gamma_2{}^L x_2)^{v_2} \qquad (6)$$

where x_i and γ_i^L are the mole fraction and activity coefficient of component C_i, and z_3 ($z_3 = 1$) refers to the mole fraction of C_3. Another expression for K_a can be derived from the Gibbs–Helmholtz equation, as shown in Equation 7[18]:

$$K_{\mathrm{a}} = K_{\mathrm{ref}} \times \exp\left[\frac{\Delta H_{\mathrm{ref}}}{RT_{\mathrm{ref}}}\left(\frac{T-T_{\mathrm{ref}}}{T}\right)\right] \qquad (7)$$

where K_{ref} and ΔH_{ref} are the equilibrium constant and enthalpy of reaction at an arbitrarily chosen reference temperature, T_{ref}. By solving Equations 6 and 7, the liquidus temperature can be determined. In the CF model, v_1 and v_2 were used as fitting parameters.

A mixture that forms molecular compounds has a liquidus line with one or more upwardly convex curves. As demonstrated in our previous study[12], such complex liquidus curves were found in MAG/MAG mixtures and could be explained well using this CF model.

3 Results and Discussion

3.1 Pure component properties

The thermal properties of the pure materials were evaluated, as shown in Table 2, and used to calculate the thermodynamic models. Experimental uncertainties in triplicate measurements were within −0.8 to +1.3 °C of the mean melting point and −2.0% to +1.1% of the mean enthalpy of fusion.

Metastable α crystal data were used for MAGs because liquidus temperatures attributed to α-type MAGs were observed under the given DSC conditions[5,12], as explained in the experimental section. Stable β_1 and β crystal data were used for DAGs and TAGs, respectively, because these materials seemed to have either transitioned rapidly during DSC measurement or crystallized directly to these stable forms while cooling. These behaviors were the same as reported in our previous study[5,12,15]. As an exception, β crystal data was used for MAG18:1 owing to the fast transition of unsaturated MAG[19], similar to DAGs and TAGs.

3.2 DSC profiles of binary mixtures

The binary mixtures exhibited some typical behaviors in DSC analysis, with examples shown in Fig. 1. When the melting point difference between the two components was large, which was the most common case in this study, a single endothermic peak was observed, as shown in Fig. 1(a) (DAG18:0/DAG18:1). This peak corresponded to the liquidus temperature of the mixture, which shifted gradually to a higher temperature as the DAG18:0 fraction increased. The solidus peak was usually not observed in this case because, as mentioned in the experimental section, the mixture was reheated immediately after the first

exothermic peak was passed in the cooling cycle, preventing the mixture from fully solidifying.

When the melting point difference was small, multiple endothermic peaks were observed, as shown in Fig. 1(b) (DAG18:0/DAG16:0). This might be due to the mixture fully solidifying in the cooling cycle, resulting in multiple melting processes appearing in the DSC profile. In this case, the highest (filled triangles) and lowest (open triangles) endothermic peak temperatures were assigned as the liquidus and solidus temperatures of the mixture, respectively. However, the peaks in Fig. 1(b) seem to be broad, containing several shoulders. This may be because the crystal transition was not completed during the analysis, and the endothermic peak attributed to both β_1 and β_2 crystals overlapped, as discussed later.

When TAG was a component in the mixture and solidified during the cooling cycle, as shown in Fig. 1(c) (DAG18:1/TAG16:0), a small exothermic peak (indicated by arrows) was observed in addition to the liquidus endothermic peak (filled triangles). This exothermic peak might be due to the rapid melt-mediated crystal transition from α to β-type TAG upon heating[20].

3.3 Binary mixtures of the same type of acylglycerol

This section covers binary mixtures of the same type of acylglycerol, namely, TAG/TAG, DAG/DAG, and MAG/MAG. As TAG/TAG and MAG/MAG pairs have been studied by us and other researchers, as mentioned later, the current study focused on DAG/DAG mixtures, with the results shown in Fig. 2. In triplicate trials, the experimental uncertainties were within −0.6 to +0.7 °C of the mean for liquidus, and −0.5 to +0.6 °C of the mean for solidus.

For the DAG18:0/DAG12:0 mixture, the experimentally determined liquidus increased monotonically with increasing DAG18:0 content, as shown in Fig. 2(a). Owing to the relatively large difference between the melting points of DAG18:0 and DAG12:0, no significant difference was observed between the NSS and SS models, such that the experimental liquidus fitted both models well. However, the measured solidus was almost constant at around 56 °C, regardless of the mole fraction. As this is a typical characteristic of eutectic systems, the actual behavior of this mixture was considered to follow the NSS model more closely.

The experimental liquidus of DAG18:0/DAG16:0, as shown in Fig. 2(b) based on the results of Fig. 1(b), was closer to the NSS model than the SS model. Furthermore, as the solidus was constant at around 63 °C, this mixture appeared to be a eutectic system, following the NSS model. The experimental liquidus tended to be slightly lower than the NSS model, which might be due to the heating time to the liquidus temperature being short in this mixture, such that the crystal transition from β_2 to β_1 was not complete. The DSC profiles in Fig. 1(b) were broad, and multiple crystal types appeared to be involved. Given this fact, the liquidus temperature, almost constant around 68 °C in the DAG18:0 content from 0.2 to 0.6, may correspond to the solidus of β_1 crystal rather than the liquidus. In this region, since the actual liquidus peak was probably small and buried in the solidus peak, the liquidus temperature could not be determined correctly from the DSC profile. The solidus temperature around 63°C could be attributed to β_2 rather than β_1. Note that the melting point of β_2-type DAG18:0 (76.8 °C) was about 3 °C lower than that of β_1 (79.6 °C).

For the DAG18:0/DAG18:1 mixture, the experimental liquidus was in good agreement with both models, as shown in Fig. 2(c). As the NSS and SS models almost overlapped due to the very large melting point difference, and no solidus was observed in this case, it was difficult to determine which model was correct for the real behavior. However, considering that other DAG/DAG mixtures follow the NSS model, it seems that DAG/DAG mixtures can generally be predicted using the NSS model. The same has also been shown for some diacid DAGs[21] and DAG16:0/DAG18:1 mixtures[22].

For TAG/TAG mixtures, a review by Timms concluded that eutectic behavior is most commonly observed[13], implying that TAG/TAG mixtures can generally be represented by the NSS model, in addition to DAG/DAG mixtures. As some exceptions, specific TAG/TAG combinations can

form molecular compounds at certain compositions[13,14]. For example, Engström reported that 2-oleo-1,3-distearin (StOSt) and 1-oleo-2,3-distearin (OStSt) form a molecular compound with a composition of approx. 1:1[23]. Zhang et al. suggested that certain combinations of fatty acid moieties of TAGs resulted in specific glycerol conformations that support compound formation[14]. However, such cases are rare, and since the TAG content in biodiesel is generally smaller than that of MAG, the effect of TAG/TAG compound formation on biodiesel CFP is considered limited. The European biodiesel standard EN14214 restricts the TAG and DAG contents to $\leq$ 0.2 wt% each and MAG content to $\leq$ 0.7 wt%[24].

Meanwhile, our recent report showed that all MAG/MAG mixtures studied had complex liquidus curves, represented only by the CF model, suggesting the formation of molecular compounds between different types of MAG[12]. Compared with TAG/TAG and DAG/DAG mixtures, MAG/MAG seems to form molecular compounds readily owing to the presence of two hydroxyl groups in the MAG molecule, which form strong intermolecular hydrogen bonding with carbonyl groups of another MAG molecule[25].

3.4 Binary mixtures of different types of acylglycerol

The solid–liquid phase behaviors of binary DAG/MAG, TAG/MAG, and DAG/TAG mixtures are shown in Figs. 3–5, respectively. The experimental uncertainties in triplicate trials were within –0.9 to +0.8 °C (liquidus) and –0.9 to +0.7 °C (solidus) of the means in Fig. 3, –0.6 to +0.9 °C (liquidus) in Fig. 4, and –0.6 to +0.7 °C (liquidus) in Fig. 5.

Among the DAG/MAG mixtures, the experimental liquidus temperatures for DAG12:0/MAG12:0 (Fig. 3(a)), DAG18:0/MAG18:0 (Fig. 3(b)), and DAG18:0/MAG18:1 (Fig. 3(c)) were clearly on the V-shape curve, in good agreement with values calculated by the NSS model. Solidus temperatures were also observed in these mixtures, with no significant change observed with different compositions. These behaviors were typical of eutectic systems.

The behavior of DAG18:0/MAG18:1, as shown in Fig. 3(d), was similar to that shown in Fig. 2(c), and the experimental liquidus values were well explained by the NSS model, despite the large difference in melting points making distinguishing between the NSS and SS models difficult.

As shown in Fig. 3(e), the DAG18:1/MAG16:0 mixture was an exception. In the region where the DAG18:1 fraction was more than 0.6, the experimental liquidus deviated to a higher temperature than the NSS model, suggesting molecular compound formation, which can be reasonably explained by the CF model. The parameters of the CF model were determined as follows: v_1 (MAG16:0) = 5.1, v_2 (DAG18:1) = 14.6, K_{ref} = 0.00016, and ΔH_{ref} = 74.4 kJ/mol. Note that these values are only the result of data fitting and do not necessarily reflect the actual values. However, even if compound formation occurs when the DAG fraction is high, its effect on the CFPs of actual biodiesel (generally, MAG content > DAG content) might not be significant. The NSS model seems to be sufficient for predicting the solidification behavior of biodiesel.

For the TAG/MAG mixtures, the experimental liquidus temperatures were on the V-shape curve for TAG18:0/MAG18:0 (small melting point difference; Fig. 4(a)), and monotonically increased for TAG18:0/MAG12:0 (Fig. 4(b)) and TAG16:0/MAG18:1 (large melting point differences; Fig. 4(c)), with no sign of compound formation. These results indicated that the TAG/MAG mixtures were also essentially eutectic or monotectic, which should be explained by the NSS model, similar to DAG/MAG mixtures. However, deviations between the NSS model and experimental values were observed, especially in the low TAG content region of Fig. 4(b). When the difference in fatty acid chain length between TAG and MAG was large, the UNIFAC (Dortmund) model tended to estimate a very large activity coefficient (γ_i^L) at low TAG contents. For example, in Fig. 4(b), the γ_i^L value was about 60 when the TAG18:0 fraction was 0.01, resulting in higher predicted liquidus temperature. The reason for this is unclear, but UNIFAC (Dortmund) might not be able to sufficiently evaluate the TAG/MAG mixtures.

For the DAG/TAG mixtures in Fig. 5, the experimental liquidus showed a slight V-shaped trend or monotonic change. Relatively good agreement with the NSS model was observed, allowing explanation by the eutectic or monotectic system, similar to other mixtures. However, as shown in Fig. 5(b), when the difference in fatty acid chain length between TAG and DAG was large, the NSS model results tended to be higher than the experimental results in the low TAG content region (high DAG content). This was also due to the $\gamma_i{}^L$ value being quite large ($\gamma_i{}^L$ = 2.5 when TAG18:0 fraction was 0.01), but not noticeable compared with that of Fig. 4(b). The evaluation of activity coefficients by UNIFAC (Dortmund) appears able to express the experimental results quite well for TAG/DAG mixtures.

As an additional discussion, enthalpy analysis was performed based on the DSC profile to determine whether the mixture with monotonically varying liquidus curve would follow the NSS or SS model. Fig. 6 shows the liquidus temperature and enthalpy of melting at liquidus of various mixtures. For DAG18:0/DAG18:1 (Fig. 6a), the enthalpy increased linearly with the DAG18:0 content. Therefore, only pure DAG18:0 crystal appeared to be melted at the liquidus temperature, meaning that this mixture is eutectic and follows the NSS model. Similarly, the enthalpy curves of the other mixtures (Figs. 6b-d) varied linearly, suggesting that they are also eutectic systems.

4 Conclusions

This study showed that the liquidus temperatures of DAG/DAG mixtures either follow a simple V-shape curve or change monotonically, both of which fit well with values predicted by the NSS model. The formation of molecular compounds between different types of DAG was not observed. According to previous studies, such eutectic or monotectic behavior has also been commonly observed in TAG/TAG mixtures. Similarly, the liquidus curves of binary mixtures of different types of acylglycerol, namely, DAG/MAG, TAG/MAG, and DAG/TAG, were in good agreement with the NSS model, with a few exceptions. However, for TAG/MAG mixtures, concerns remained regarding the reliability of the UNIFAC (Dortmund) model for estimating the activity coefficient. These results implied that each component solidified independently as a pure substance in the above mixtures. This contrasted with the results of our previous study on MAG/MAG mixtures, whose liquidus curves were very complex, showing a strong tendency to form molecular compounds described only by the CF model. As the MAG content in biodiesel is generally higher than that of DAG and TAG, and MAG is less likely to form molecular compounds with TAG and DAG, it can be assumed that the effect of DAG and TAG on biodiesel CFPs is limited. Therefore, to accurately predict the biodiesel CFPs, understanding the behavior of MAG, especially its molecular compound formation, is probably important.

Acknowledgement

We thank Simon Partridge, PhD, from Edanz Group for editing a draft of this manuscript.

Conflict of Interest

The authors have declared no conflict of interest.

References

[1] L. Yu, I. Lee, E. G. Hammond, L. A. Johnson, J. H. Van Gerpen. The influence of trace components on the melting point of methyl soyate. *J. Am. Oil Chem. Soc.*, **1998**, *75*, 1821–1824.

[2] H. Tang, R. C. De Guzman, S. O. Salley, K. Y. S. Ng. Formation of insolubles in palm oil-, yellow grease-, and soybean oil-based biodiesel blends after cold soaking at 4 °c. *J. Am. Oil Chem. Soc.*, **2008**, *85*, 1173–1182.

[3] G. M. Chupka, J. Yanowitz, G. Chiu, T. L. Alleman, R. L. McCormick. Effect of saturated monoglyceride polymorphism on low-temperature performance of biodiesel. *Energy Fuels*, **2011**, *25*, 398–405.

[4] Y. Sugami, S. Yoshidomi, E. Minami, N. Shisa, H. Hayashi, S. Saka. The effect of monoglyceride polymorphism on cold-flow properties of biodiesel model fuel. *J. Am. Oil Chem. Soc.*, **2017**, *94*, 1095–1100.

[5] S. Yoshidomi, Y. Sugami, E. Minami, N. Shisa, H. Hayashi, S. Saka. Predicting solid–liquid equilibrium of fatty acid methyl ester and monoglyceride mixtures as biodiesel model fuels. *J. Am. Oil Chem. Soc.*, **2017**, *94*, 1087–

1094.
[6] I. Foubert, K. Dewettinck, D. Van de Walle, A. J. Dijkstra, P. J. Quinn. Physical properties: Structural and physical characteristics, in *Lipid Handb. with CD-ROM*, (Eds: F.D. Gunstone, J.L. Harwood, A.J. Dijkstra), CRC Press, Boca Raton, **2007**.
[7] I. Paryanto, T. Prakoso, M. Gozan. Determination of the upper limit of monoglyceride content in biodiesel for B30 implementation based on the measurement of the precipitate in a Biodiesel–Petrodiesel fuel blend (BXX). *Fuel*, **2019**, *258*, 116104.
[8] H. Imahara, E. Minami, S. Saka. Thermodynamic study on cloud point of biodiesel with its fatty acid composition. *Fuel*, **2006**, *85*, 1666–1670.
[9] R. O. Dunn. Crystallization behavior of fatty acid methyl esters. *J. Am. Oil Chem. Soc.*, **2008**, *85*, 961–972.
[10] J. C. A. Lopes, L. Boros, M. A. Kráhenbúhl, A. J. A. Meirelles, J. L. Daridon, J. Pauly, I. M. Marrucho, J. A. P. Coutinho. Prediction of cloud points of biodiesel. *Energy and Fuels*, **2008**, *22*, 747–752.
[11] R. O. Dunn. Correlating the Cloud Point of Biodiesel to the Concentration and Melting Properties of the Component Fatty Acid Methyl Esters. *Energy and Fuels*, **2018**, *32*, 455–464.
[12] L. Seniorita, E. Minami, Y. Yazawa, H. Hayashi, S. Saka. Differential Scanning Calorimetric Study of Solidification Behavior of Monoacylglycerols to Investigate the Cold-Flow Properties of Biodiesel. *J. Am. Oil Chem. Soc.*, **2019**, *96*, 979–987.
[13] R. E. Timms. Phase behaviour of fats and their mixtures. *Prog. Lipid Res.*, **1984**, *23*, 1–38.
[14] L. Zhang, S. Ueno, K. Sato. Binary phase behavior of saturated-unsaturated mixed-acid triacylglycerols—A review. *J. Oleo Sci.*, **2018**, *67*, 679–687.
[15] L. Seniorita, E. Minami, H. Kawamoto. Solidification behavior of acylglycerols in fatty acid methyl esters and effects on the cold flow properties of biodiesel. *J. Am. Oil Chem. Soc.*, **2021**, *98*, 727–735.
[16] J. M. Smith, H. C. Van Ness, M. M. Abbott. *Introduction to Chemical Engineering Thermodynamics*, McGraw-Hill Education, New York, **2005**.
[17] J. Gmehling, J. Li, M. Schiller. A modified UNIFAC model. 2. Present parameter matrix and results for different thermodynamic properties. *Ind. Eng. Chem. Res.*, **1993**, *32*, 178–193.
[18] J. M. Prausnitz, R. N. Lichtenthaler, E. G. de Azevedo. *Molecular Thermodynamics of Fluid-Phase Equilibria*, Prentice Hall PTR, New Jersey, **1999**.
[19] J. Vereecken, W. Meeussen, I. Foubert, A. Lesaffer, J. Wouters, K. Dewettinck. Comparing the crystallization and polymorphic behaviour of saturated and unsaturated monoglycerides. *Food Res. Int.*, **2009**, *42*, 1415–1425.
[20] K. Sato, T. Kuroda. Kinetics of melt crystallization and transformation of tripalmitin polymorphs. *J. Am. Oil Chem. Soc.*, **1987**, *64*, 124–127.
[21] R. J. Craven, R. W. Lencki. Binary phase behavior of diacid 1,3-diacylglycerols. *J. Am. Oil Chem. Soc.*, **2011**, *88*, 1125–1134.
[22] Y. Xu, C. Dong. Phase behavior of binary mixtures of three different 1,3-diacylglycerols. *Eur. J. Lipid Sci. Technol.*, **2017**, *119*, 1–13.
[23] L. Engström. Triglyceride systems forming molecular compounds. *Eur. J. Lipid Sci. Tech.*, **1992**, *94*, 173–181.
[24] Committee for Standardization Automotive Fuels. *Fatty Acid Methyl Esters (FAME) for Biodiesel Engines - Requirements and Test Methods (EN14214)*, European Committee For Standardization CEN, **2008**.
[25] A. Holmgren, G. Lindblom, L. B. . Johansson. Intramolecular hydrogen bonding in a monoglyceride lipid studied by Fourier transform infrared spectroscopy. *J. Phys. Chem.*, **1988**, *92*, 5639–5642.

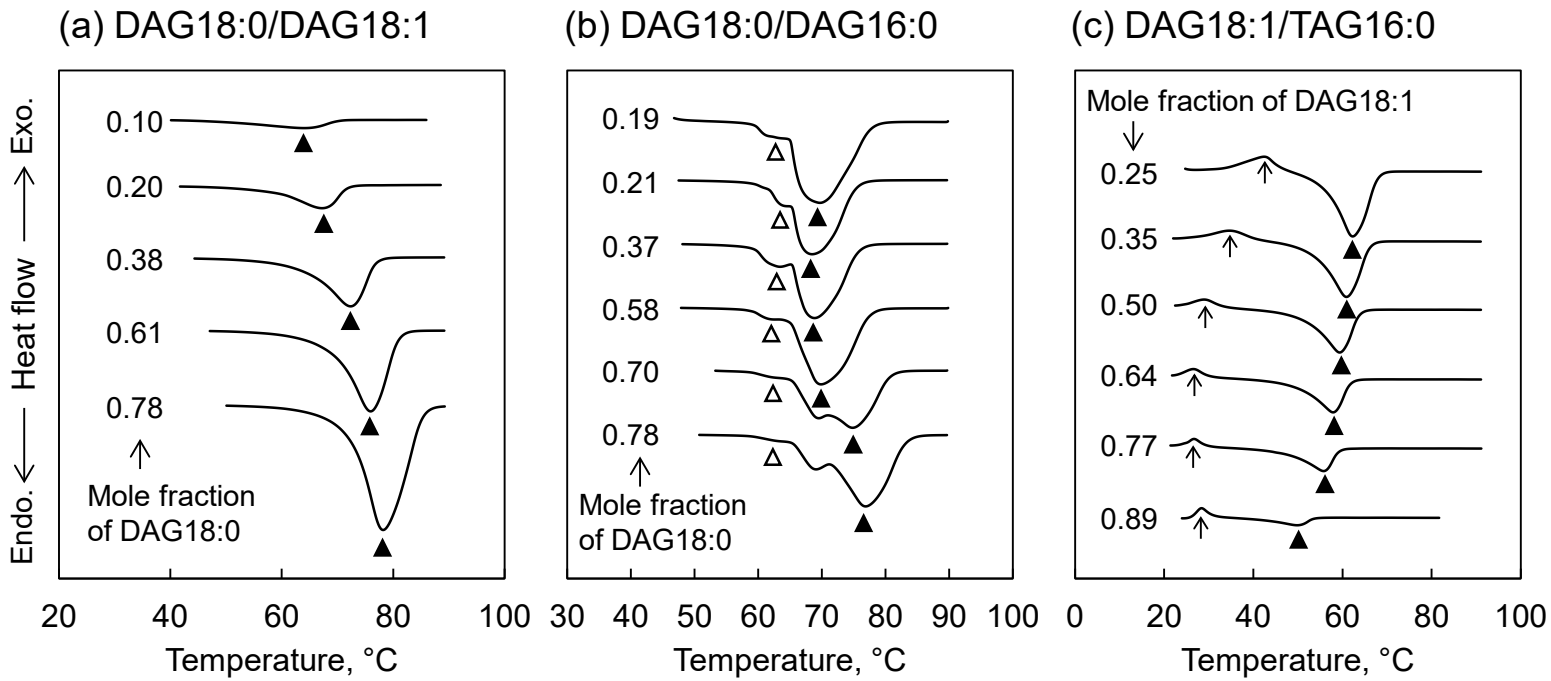

Fig. 1. DSC profiles at a heating rate of 10 °C/min for mixtures of (a) DAG18:0/DAG18:1, (b) DAG18:0/DAG16:0, and (c) DAG18:1/TAG16:0 at various mole fractions. Filled and open triangles indicate the liquidus and solidus peaks, respectively.

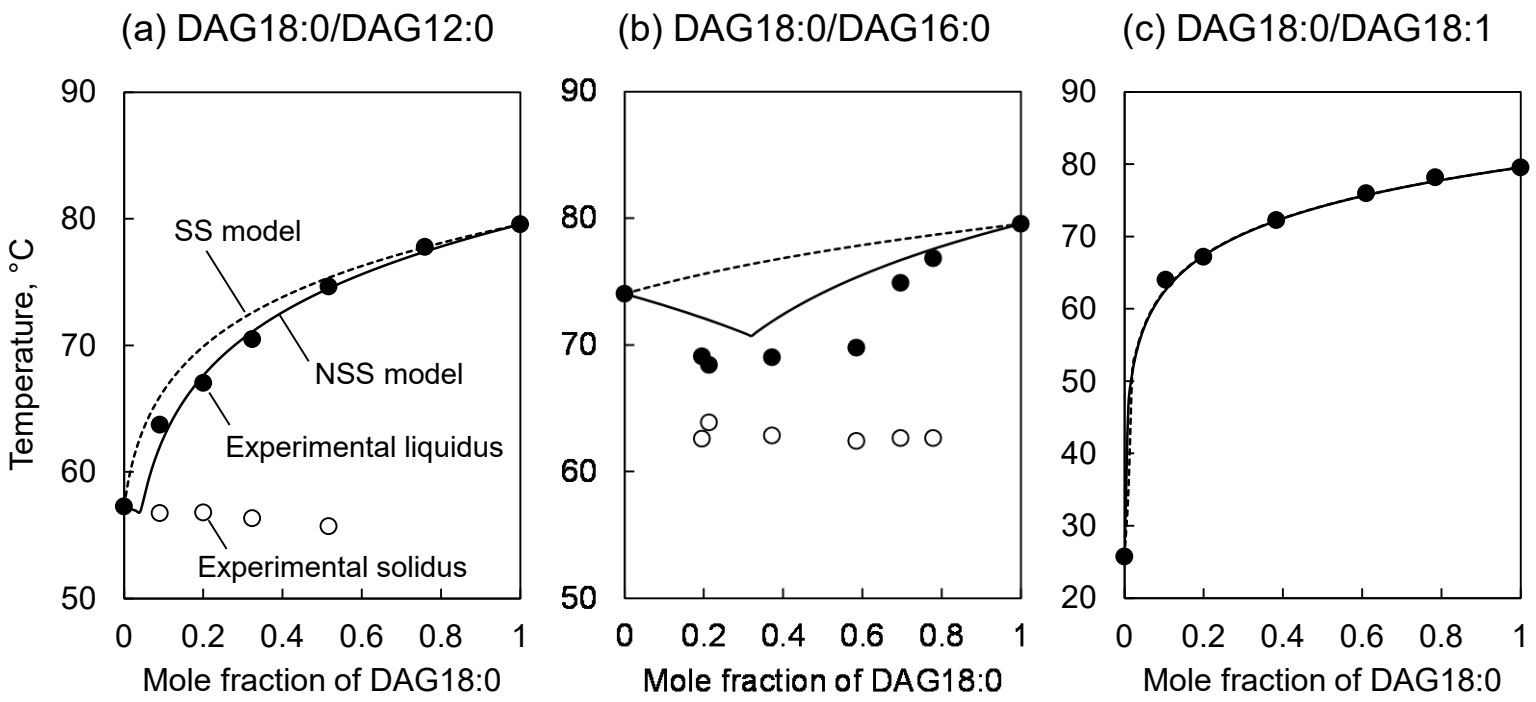

Fig. 2. Experimentally determined liquidus (filled circles) and solidus (open circles) temperatures of various DAG/DAG binary mixtures, and theoretical liquidus curves calculated using the NSS (solid line) and SS (dashed line) models.

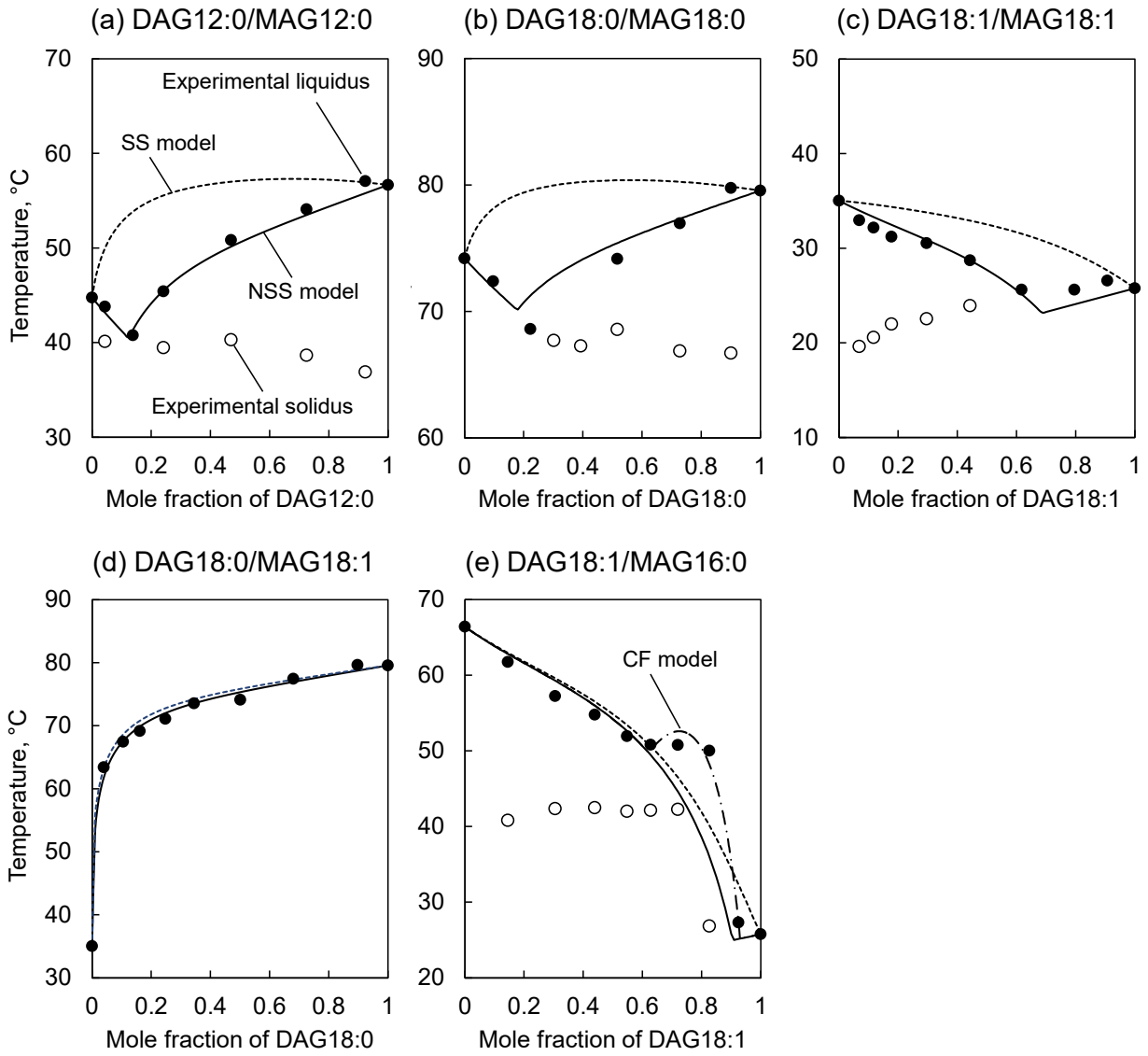

Fig. 3. Experimentally determined liquidus (filled circles) and solidus (open circles) temperatures of various DAG/MAG binary mixtures, and theoretical liquidus curves calculated using the NSS (solid line), SS (dashed line), and CF (dashed-dotted line) models.

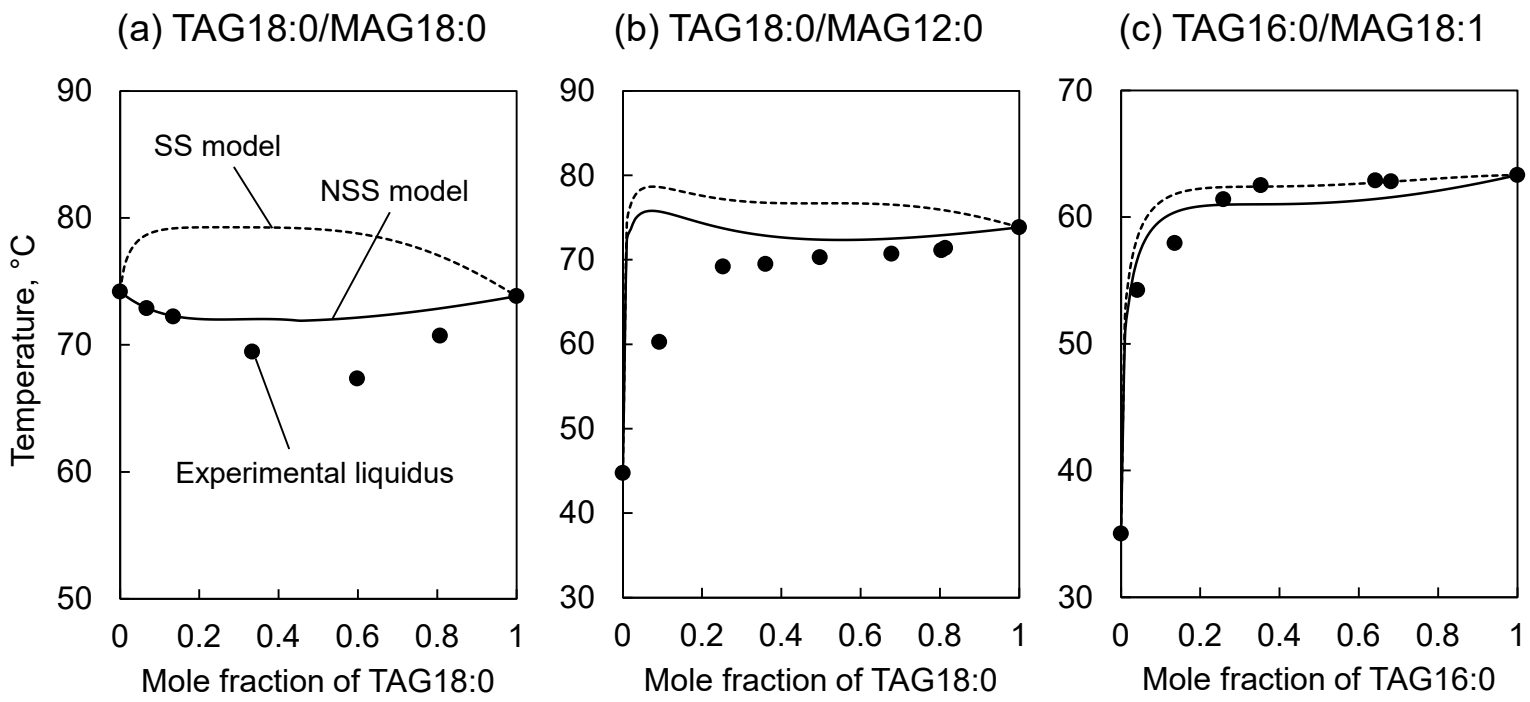

Fig. 4. Experimentally determined liquidus (filled circles) temperatures of various TAG/MAG binary mixtures, and theoretical liquidus curves calculated using the NSS (solid line) and SS (dashed line) models.

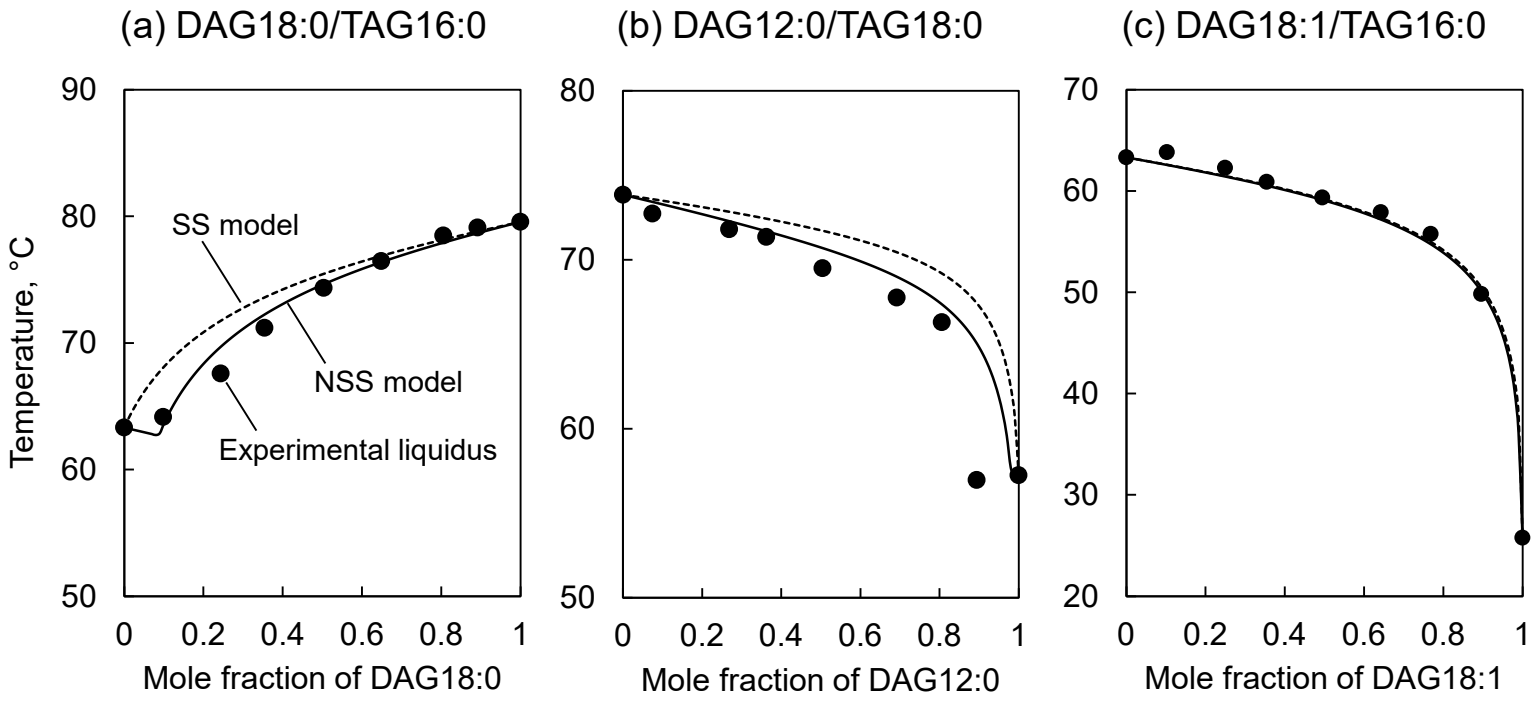

Fig. 5. Experimentally determined liquidus (filled circles) temperatures of various DAG/TAG binary mixtures, and theoretical liquidus curves calculated using the NSS (solid line) and SS (dashed line) models.

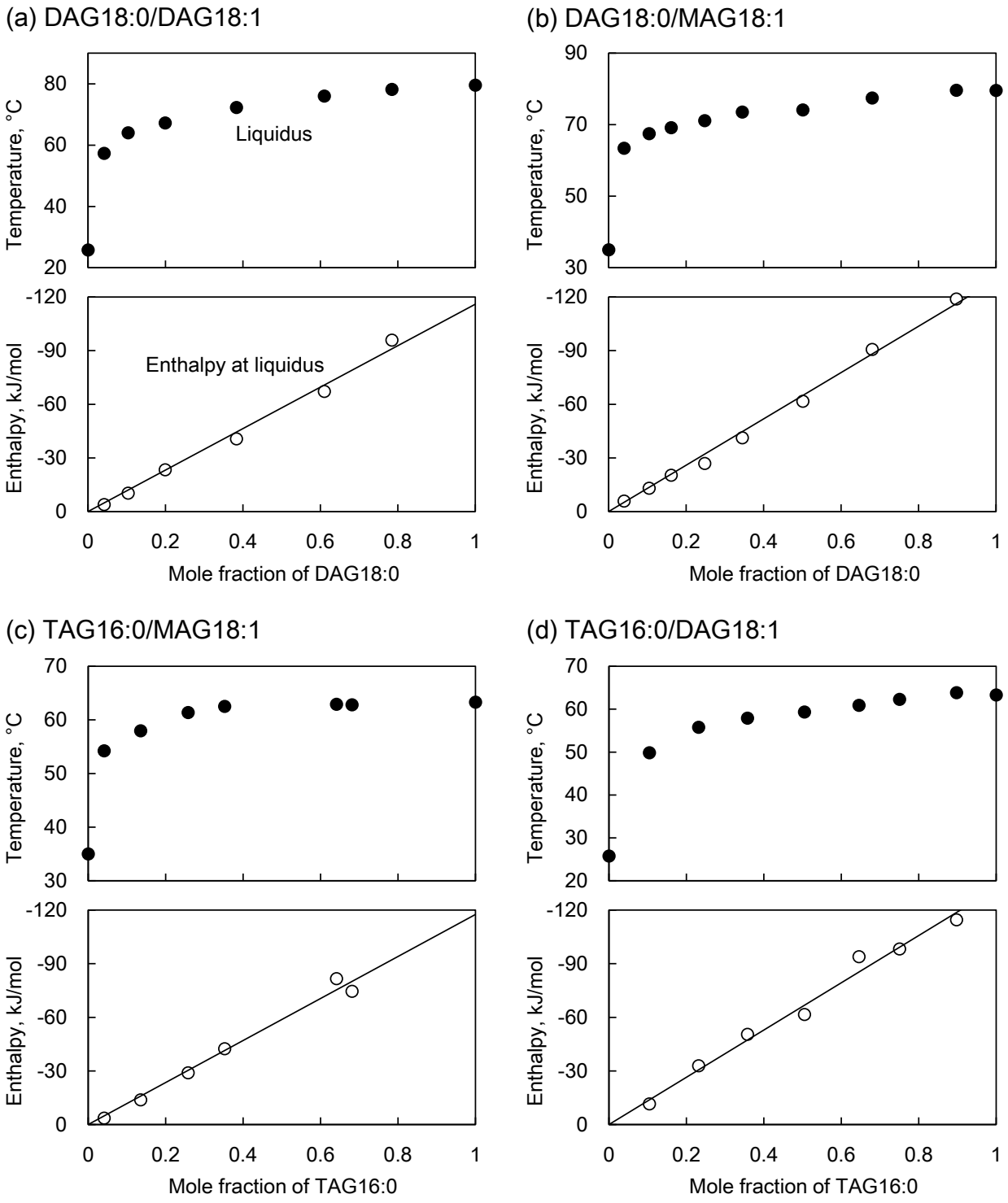

Fig. 6. Experimentally determined liquidus temperatures (filled circles) and enthalpies of melting at liquidus (open circles) for various binary mixtures.